LITERATURE CITED

1. L. I. Sedov, The Methods of Similarity and Dimensionality in Mechanics [in Russian], Nauka, Moscow (1981).
2. V. P. Korobeinikov, Problems in the Theory of a Spot Explosion [in Russian], Nauka, Moscow (1985).
3. T. E. Andreeva, S. I. Gritsinin, I. A. Kossyi, et al., "Relaxation of vibrationally excited nitrogen with consideration of gasdynamics phenomena," Brief Communications in Physics, No. 7 (1983).
4. V. A. Gasilov, V. Ya. Karpov, A. Yu. Krukovskii, et al., "Calculating the development of an axisymmetric thermal explosion in a molecular gas," Preprint, IVTAN, No. 5-138, Moscow (1984).
5. A. L. Vikharev, M. S. Gitlin, O. A. Ivanov, et al., "The heating of nitrogen in a pulsed SHF discharge under conditions of intensive excitation of molecular electron levels," Pis'ma Zh. Tekh. Fiz., 13, No. 4 (1987).
6. A. Kh. Mnatsakanyan and G. V. Naidis, "Difference methods for the solution of gasdynamic problems," Teplofiz. Vys. Temp., 23, No. 4 (1985).
7. A. A. Samarskii and Yu. P. Popov, Difference Methods of Solution of Gasdynamic Problems [in Russian], Nauka, Moscow (1980).
8. H. Honma and I. I. Glass, "Weak spherical shock-wave transitions of N-waves in air with vibrational excitation," Proc. R. Soc. London, A391, No. 1800 (1984).
9. Ya. B. Zel'dovich and Yu. P. Raizer, The Physics of Shock Waves and High-Temperature Hydrodynamic Phenomena [in Russian], Nauka, Moscow (1966).

# THE FORMATION OF SHOCK WAVES WITH AN EXPLOSIVE PROFILE IN A SHOCK TUBE

M. K. Berezkina, I. V. Smirnov, and M. P. Syshchikova UDC 533.6.011.72:534.222.2

A plane shock wave (SW) with a variable pressure profile behind the front can be produced in a shock tube of constant cross section, with a diaphragm, at the point at which the SW front overtakes the rarefaction wave (RW), reflected from the end of a high-pressure chamber (HPC).

Based on a numerical model of the flow which occurs in the explosion of a layer which can be represented as a flow that is achieved in a shock tube in the case of the instantaneous removal of the diaphragm, it has been demonstrated in [1] that there exists such values of the determining parameters that the pressure at the front of the SW at the instant at which the head of the RW is overtaken is close to the pressure at the front of the SW in the case of a point plane explosion. Further changes in the pressure at the front of the SW are also close to the relationship between the pressure at the front of the SW and the distance for the point explosion. Given other values for the determining parameters, the pressure at the front of the SW at the instant of overtaking the RW is smaller than the pressure of the point explosion and approach to the quantitative relationship governing the point explosion occurs at a distance exceeding the distance required to overtake the other wave.

At the present time the model of the point explosion has been studied more thoroughly [2] and in many cases provides an excellent description of the problem of real explosions. The interrelationship of the parameters of a SW formed in a shock tube after the RW has been overtaken with the parameters of the SW in the case of a point explosion, such as observed in numerical modeling [1], is deserving of attention. We have the possibility of using installations of this kind to model the processes of interaction between bodies and the waves from an explosion.

Leningrad. Translated from Zhurnal Prikladnoi Mekhaniki i Tekhnicheskoi Fiziki, Vol. 30, No. 6, pp. 50-56, November-December, 1989. Original article submitted July 15, 1988.

 

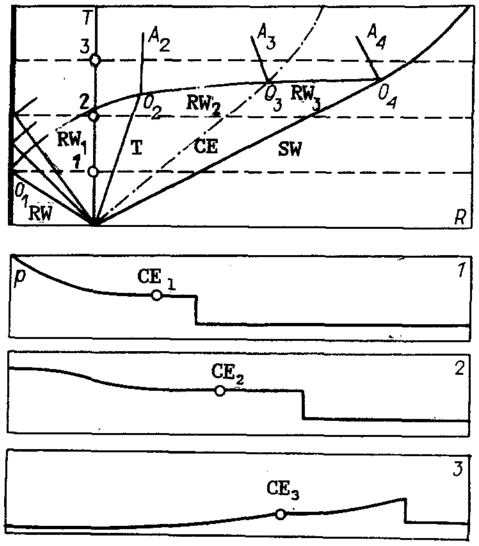


Fig. 1

The experimental investigation of the flow in a shock wave of constant cross section was conducted, as a rule, either in that segment where the velocity of the SW front increases due to the noninstantaneity of diaphragm explosion [3, 4], or in that segment where the velocity of the front undergoes virtually no change, while the parameters of the gas behind the front are constant [4, 5]. Investigations into the flow in later stages, where the head of the RW, reflected from the face of the HPC, overtakes the front of the SW, are virtually nonexistent [6].

In the present study, based on numerical and physical models, we examine the quantitative relationships involved in the formation and propagation of plane SW with a variable pressure profile in the shock tube. We undertake a comparison of the calculations carried out in accordance with the ideal theory of a shock tube and for the model of a point explosion.

1. Determining Parameters. Figure 1 shows a diagram of the flow that is set up in a shock tube in the case of the instanteous removal of the diaphragm, as well as the distribution of pressure in space for three characteristic instants of time. At the instant of time 1 the pressure behind the SW front in two regions separated by a contact explosion ($CE_1$) continuously and smoothly increases into a RW to a maximum value at the wall. In the subsequent instants of time the basic changes in the flow are associated with the propagation of the head of the $RW_1$ propagated through the channel and reflected from the end of the HPC, and its interaction with the tail (T) at point $O_2$, with the CE at point $O_3$, and with the front of the initial SW at point $O_4$. In the interaction of $RW_2$ with CE at point $O_3$ a passing $RW_3$ and a reflected wave $A_3$ are formed, the latter being either a RW or a SW, formed out of compression waves. The velocity of the CE after interaction with $RW_2$ begins to diminish and at the limit, when the pressure at the CE becomes commensurate with the initial pressure, turns out to be equal to zero. At the point at which the rarefaction wave overtakes the initial SW the pressure behind the front ceases to be constant, and at the boundary separating the two gases of the $CE_3$ (instant of time 3) the pressure curve undergoes a break.

The gasdynamic parameters of the flow in the shock tube are functions of the spatial R and time T variables, as well as of the initial parameters $p_d$, $a_d$, k, $\gamma_0$ ($p_d$ and $a_d$ are the initial ratio of the pressures at the diaphragm and the ratios of the speeds of sound in the HPC and in the low-pressure channel (LPC), with k and $\gamma_0$ representing the adiabatic exponents in the HPC and LPC). For the scales of the spatial and time variables we have $R^0 = r_d'$, $T^0 = r_d'\sqrt{\gamma_0}/a_0$ ($r_d'$ is the length of the HPC, and $a_0$ is the initial speed of sound in the LPC).

When we compare the flow in the shock tube with the flow which arises in a point explosion, it is convenient to use another system of determining parameters: $r_d$, $a_d$, k, $\gamma_0$ ($r_d$ is the dimensionless length of the HPC). In this case, for the spatial $r^0$ and time $t^0$ scales, as in the theory of point explosion, we specify

$$r^0 = \frac{E_0}{p_0\alpha^0} = \frac{2p_d r_d'}{(k-1)\,\alpha^0}, \quad t^0 = \frac{r^0\sqrt{\gamma_0}}{a_0},$$

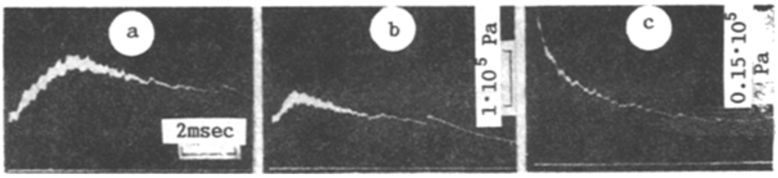


Fig. 2

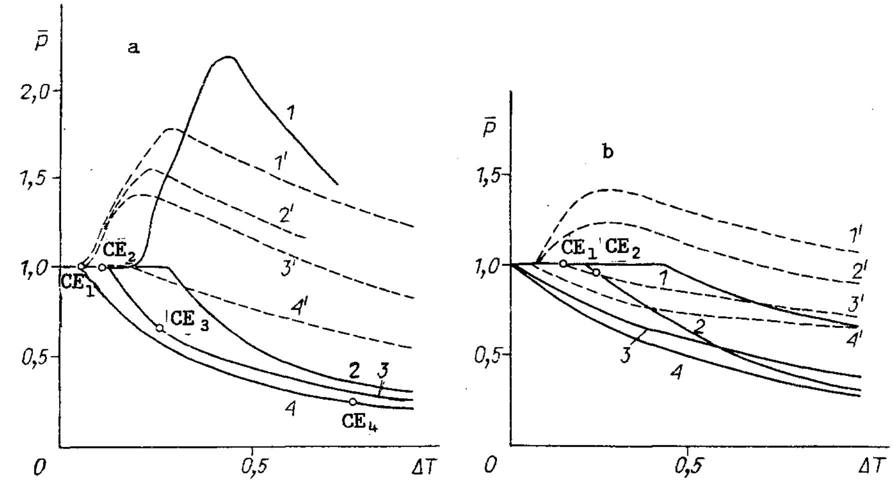


Fig. 3

where $E_0$ is the energy of the compressed gas in the HPC (or the energy of the explosion); $\alpha^0$ is the self-similar constant which is dependent on the $\gamma_0$ of the medium and the symmetry of motion [2], with $\gamma_0 = 1.4$ $\alpha^0 = 1.077$; $p_0$ is the initial pressure in the LPC. The dimensionless length of the HPC in these variables proves to be equal to

$$r_d = \frac{r'_d}{r^0} = \frac{(k-1)}{2p_d}\alpha^0,$$

while the relationship between the physical R, T and the dynamic r, t variables is determined by the relationships $r = r_d R$, $t = r_d T$.

2. Experimental Method. The experiments were conducted with a shock tube of rectangular cross section 50 × 150 mm. The overall length of the installation was 12 m. The LPC is 9 m in length and consists of individual steel sections, the HPC are demountable and are 85 mm, 1 and 2 m in length. The separation diaphragms were made of copper strip with thicknesses of 0.15, 0.25, and 0.4 mm. Special shears were used to notch the diaphragms.

We studied the real flow in the shock tube in relation to the initial parameters: $p_d$, $a_d$, k, and $\gamma_0$. The basic quantities that we measured included the velocity of the SW front and the pressure profile behind that front, and these were recorded at a fixed point in the channel with various HPC lengths. The dimensionless distance of the point of observation from the end of the HPC was 4.6, 8, and 101 with $r_d' = 2$, 1 m, and 85 mm. The channel was filled with nitrogen, while the HPC was filled with either nitrogen or hydrogen. When using nitrogen as the propelling gas we have $a_d = 1$, while in the case of hydrogen we have $a_d = 3.73$. For all of the experiments $k = \gamma_0 = 1.4$.

A base method was used to determine the velocity of the SW front. The error in the determination of the Mach number $M_f$ of the SW front did not exceed 1%. To measure the pressure pulse behind the SW fronts propagating through the channel, we used piezosensors with a shielded temperature coating, such as those developed by G. N. Suntsov [7]. The signals from the piezosensors were recorded on an S8-17 memory oscillograph through an emitter repeater with a field transistor [8]. The coefficient of sensitivity for the piezosensor with a self-capacitance of 910 pF was 3 μV/Pa, while the period of the observed noise was 3.3 μsec. The dynamic error of the piezosensor (the ratio of half the noise amplitude to the

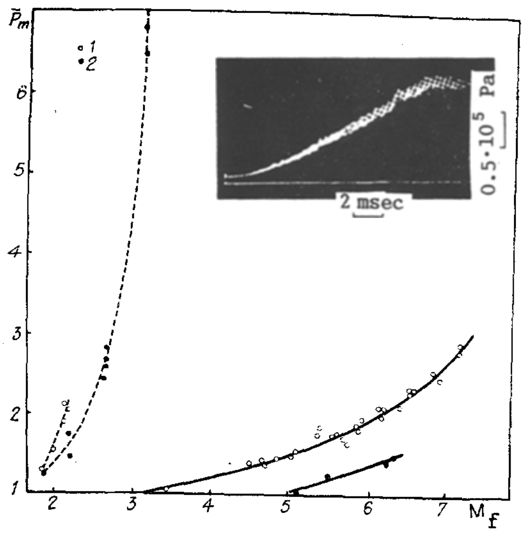


Fig. 4

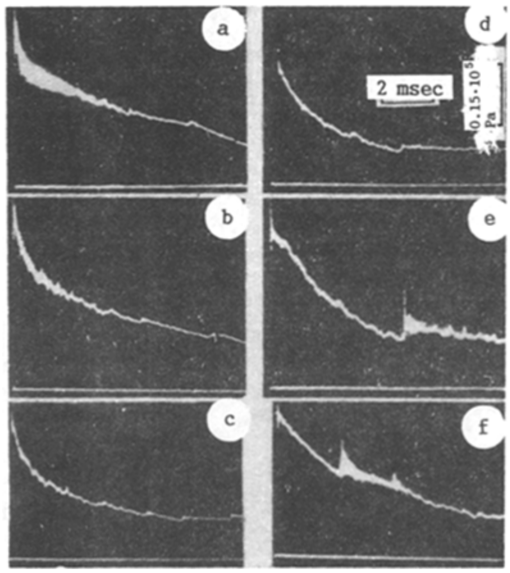


Fig. 5

TABLE 1

| No. | $p_d$ | $M_{f0}$ | $p_{f0}$ | $M_f$ | $p_f$ | No. | $p_d$ | $M_{f0}$ | $p_{f0}$ | $R$ |
|---|---|---|---|---|---|---|---|---|---|---|
| Experiment | | | | | | Theory | | | | |
| When $R = 4,6$ | | | | | | | | | | |
| 1′ | 498 | 6,48 | 48,77 | 5,38 | 33,7 | 1 | 3200 | 9,0 | 94,29 | 4 |
| 2′ | 372 | 6,09 | 43,09 | 5,10 | 30,2 | 2 | 350 | 6,0 | 41,81 | 4,6 |
| 3′ | 220 | 5,42 | 34,09 | 4,49 | 23,3 | 3 | 55 | 3,8 | 16,68 | 4,6 |
| 4′ | 73 | 4,1 | 19,44 | 3,45 | 13,7 | 4 | 25 | 3,0 | 10,33 | 4,6 |
| When $R = 8$ | | | | | | | | | | |
| 1′ | 938 | 7,32 | 62,36 | 6,26 | 45,6 | 1 | 3200 | 9,0 | 94,29 | 8 |
| 2′ | 500 | 6,48 | 48,86 | 5,51 | 35,2 | 2 | 350 | 6,0 | 41,81 | 8 |
| 3′ | 300 | 5,81 | 39,22 | 5,11 | 30,3 | 3 | 55 | 3,6 | 14,96 | 8 |
| 4′ | 220 | 5,42 | 34,09 | 4,62 | 24,7 | 4 | 25 | 2,6 | 7,72 | 8 |

signal amplitude) depends on the relationship of n between the time of SW passage past the receiving surface and the period of the observed noises [9]. The dynamic error for $n \sim 2$ amounts to 10%, and with a reduction in n it increases markedly. The time constant of the recording system allows us to conduct observations of the nonsteady pressure without distortion for 10 msec.

3. Experimental Results. The nature of the change in pressure over time behind the SW front in the hot and cold zones of the flow depends significantly on the relationship $R = R'/r_d'$ ($R'$ is the dimensional distance from the end of the HPC to the measuring section). Figure 2 shows typical pressure oscillograms obtained under identical conditions at the diaphragm, i.e., $p_d = 930$ and $a_d = 3.73$, and here R = 4.6, 8, and 101 (a-c), $M_f$ = 6.20, 6.26, and 3.51. With small values of R (Fig. 2a, b) the pressure immediately behind the front is constant over some length of time. When the tail of the RW arrives, the pressure in the cold zone of the flow begins to increase, and this ceases with the appearance in the working section of the reflected head of the RW. The peak pressure observed in the cold zone of the flow diminishes with increasing R. The nature of the change in pressure with large R is shown in Fig. 2c. In this case, at the instant at which the SW reaches the working section, its intensity drops off to $M_f = 3.51$, while the pressure behind the front drops continuously. We will present the results from the measurement of the pressure behind the SW front as a function of $p_d$ for $a_d = 3.73$ when $R \leq R_S$ and $R \gg R_S$ ($R_S$ is the dimensionless coordinate for the overtaking of the SW front by the RW).

The profiles of the pressure behind the SW front when R = 4.6 and 8 ($R \simeq R_S$) are shown, respectively, in Fig. 3a and b. Here $\bar{P} = p/p_f$ ($p_f$ and p are the pressure at the front and the instantaneous pressure behind the front). The time $\Delta T$ is calculated from the instant at which the SW reached the working section. Lines 1'-4' represent the profiles of the pressures measured experimentally, while lines 1-4 are those calculated on the basis of ideal shock-tube theory. The initial conditions for the experiment and of theory in Fig. 3 are shown in Table 1. This table shows the frontal parameters $M_{f_0}$ and $p_{f_0}$ calculated on the basis of the initial conditions, as well as the measured parameters $M_f$, $p_f$. Comparison of experiments to theory shows a marked divergence in the change of pressure within the cold zone of the flow. Let us compare two pressure profiles 2' and 2 in Fig. 3a with similar values of $p_d \sim 360$ at a distance of R = 4.6. In the experiment (profile 2') the tail of the RW is the first to arrive at this section, subsequent to which a rise in pressure is recorded. When the reflected head of the RW comes in, the pressure begins to drop. In the calculation (profile 2) we have no rise in pressure, but note only a drop in the pressure, since it is the reflected head of the RW that is the first to reach this section.

Our experiments and the results from [10] show that the time measured for the appearance of the head of the RW at a fixed section, after the descending SW has passed this point, is in good agreement with that calculated on the basis of ideal shock-tube theory. No information exists in the literature with respect to the time for the appearance of the RW tail. In the present study we have recorded a strong divergence between theory and experiment with regard to the time of the appearance of the tail at a fixed section. The tail shows up considerably earlier than predicted by theory. And here, the time for the appearance is virtually independent of the $M_f$ of the descending SW, while the time for the appearance of the head increases as $M_f$ increases. The value for the maximum pressure $\bar{P}_m$, observed in the experiment in the cold zone of the flow, also increases as $M_f$ rises.

Figure 4 shows the relationship between $\bar{P}_m = p_m/p_f$ and $M_f$, measured at the fixed section; the points connected by the dashed lines have been obtained for $a_d = 1$, while those connected by solid lines have been obtained for $a_d = 3.73$ (1, $r_d' = 2$ m and R = 4.6; 2, $r_d' = 1$ m and R = 8). Using this graph we can determine $M_f^*$ at which, at the fixed section, we have the simultaneous arrival of the tail and the head of the RW ($\bar{P}_m = 1$). For $a_d = 3.73$, $M_f^* \sim 3.2$ in the section R = 4.6 and $M_f^* \sim 5$ in the section R = 8. Then, with $M_f < M_f^*$ in the working section there is no increase in pressure in the cold zone of the flow when we compare it to the pressure at the front of the SW, while when $M_f > M_f^*$ such an increase is observed. We find a marked increase in the pressure in the cold zone of the flow with $M_f$ close to the limit values attained in the experiment. Figure 4 shows an oscillogram of the pressure for the case in which R = 4.6 when $a_d = 1$, $M_f = 3.1$, $P_f = 11.1$. The maximum pressure exceeds the pressure at the front by a factor of 12. When we conduct our studies on shock tubes we must choose the conditions of the experiments in such a manner that the rise in pressure in the flow in the working section be kept to a minimum.

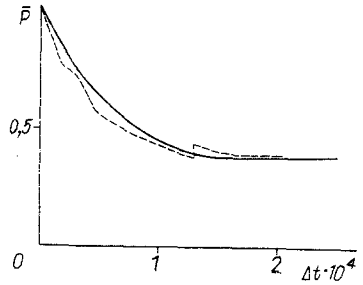


Fig. 6

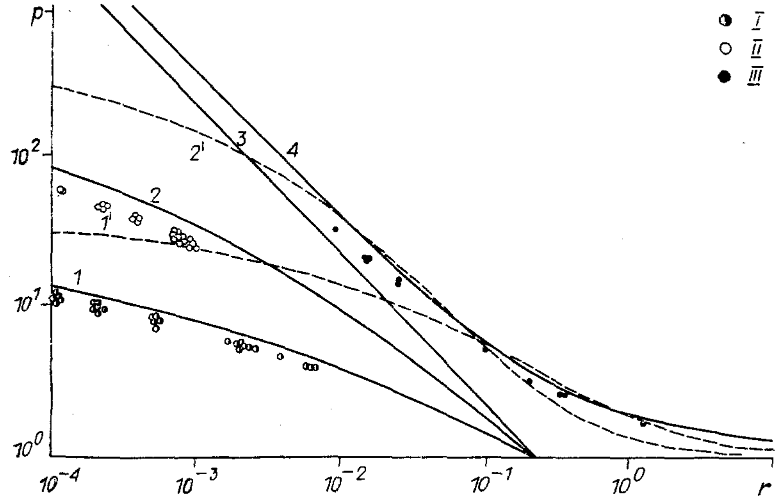


Fig. 7

The results from the measurement of pressure over time behind the front of the SW for the case in which $R \gg R_S$ are shown in Fig. 5 (a, $M_f = 4.19$, $p_f = 31.3$; b, $M_f = 4.16$, $p_f = 20.0$; c, $m_f = 3.51$, $p_f = 14.2$; d, $M_f = 2.62$, $p_f = 7.8$; e, $M_f = 2.13$, $p_f = 5.1$; f, $M_f = 1.52$, $p_f = 2.53$). In this series of experiments $r_d' = 85$ mm, $R' = 8.6$ m, which corresponds to $R = 101$. These data demonstrate the possibility of obtaining an SW of variable profile in a shock tube with a pressure drop in the zone of up to 50-70%. In certain regimes in the experiment we recorded a second SW (e, f), moving through the channel from the side of the HPC in the flow behind the initial SW. The direction of propagation for the second SW was determined from the readings of two pressure sensors positioned near each other. The second wave appears in the working section all the more rapidly, the lower the intensity of the initial SW.

Figure 6 shows a comparison of the pressure profile obtained in the shock tube (dashed line, $p_f = 6.38$) with the profile calculated on the basis of ideal shock-tube theory (solid line, $p_f = 6.54$). The pressure profile, measured in the experiment, is in rather good agreement with the theoretical calculations. The fundamental difference between theory and experiment lies in the fact that in the real flow of a shock tube we observe a second SW, the cause of whose formation has not yet been ascertained. Let us examine the parameters of the SW generated in the shock tube with the SW parameters of a point explosion in a uniform atmosphere.

Figure 7 shows the change in the pressure $p_f$ at the front of the SW with the distance r measured from the end of the HPC (or from the center of the explosion). Here 1-3 represent the calculation of $p_{fd}$ for $r = r_d$, while 1', 2' represent the calculation of $p_{fS}$ for $r = r_S$ ($r_S$ is the dimensionless coordinate for the overtaking of the front of the SW by the rarefaction wave). The calculation was based on the ideal shock-tube theory for $k = \gamma_0 = 1.4$ for all possible $p_d$, and the calculations of 1, 1', 2, 2', and 3 were based on the analytical formulas from [11] for $a_d = 1$, 3.73, and $\infty$. Curve 4 represents the calculation of $p_f$ with ($\gamma_0 = 1.4$) representing the distance from the center of the explosion in the case of a plane point explosion [2]. Functions 1, 2 yield the values of the pressure at the front of the SW in the initial segment for a given ratio of the speeds of sound within the channel and the chamber, as functions of the pressure drop $p_d$ across the diaphragm. Since as $a_d \to \infty$, $p_{fd} = p_d$ for any $r_d$, line 3 yields the relationship between $p_d$ and $r_d$. Points I and II show the values of $p_{fd}$ for $r = r_d$ when $k = \gamma_0 = 1.4$, $a_d = 1$ and 3.73, respectively, while points III indicate the pressure at the front of the SW in the segment where the waves overtake one another ($r > r_S$) for the case in which $k = \gamma_0 = 1.4$, $a_d = 3.73$ for various $p_d$. A quantitative relationship governs the change in pressure at the fronts of the SW generated in the shock tube (points III), with a distance close to that specified by the quantitative relationship governing the point explosion. The absolute values for the pressure at the front of the SW differ from those that have been calculated by an order of magnitude such as in the initial segment where the pressure behind the front is constant (points II).

Thus, in accordance with the data from numerical modeling in a real shock tube, under specific initial conditions at a distance R ~ 100 SW are formed, and their dynamics are well described by the solution of the problem of a point explosion in a medium with counterpressure. Experimentally we have produced SW of an explosion profile with differing intensities, whose $M_f$ changes over a range of 1.5-5.2 for $a_d = 3.73$ when $p_d = 63$-2400.

At a distance R ~ 1-10 we observe a significant elevation of the experimentally measured pressure (in the cold zone) over that calculated theoretically, and this is associated with the more rapid arrival of the RW tail than had been predicted by theory. We know that the experimentally measured parameters such as $M_f$ and the duration of the hot flow zone are always smaller than those indicated by theoretical calculations. The observed inverse relationship between the experimental and theoretical calculations for the pressure in the cold zone of the flow indicates that the energy stored in the HPC is transmitted less effectively to the SW than is predicted by the ideal theory of a shock tube. The observed excess of pressure in the cold flow zone over that theoretically calculated is, in all probability, caused by the fact that the diaphragm does not open instantaneously.

## LITERATURE CITED


1. E. V. Nazarov and M. P. Syshchikova, "The unique features of the dynamics of a shock wave in the explosion of a layer," Preprint No. 1100, FTI, AN SSSR, Leningrad (1987).
2. Kh. S. Kestenboim, G. S. Roslyakov, and L. A. Chudov, The Point Explosion [in Russian], Nauka, Moscow (1974).
3. L. S. Shtemenko, "The origin of shock waves in a shock tube during the process of diaphragm opening," Vestn. MGU, Ser. 3, Fizika, astronomiya, 23, No. 3 (1982).
4. I. Glass and G. Patterson, "A theoretical and experimental study of flows in a shock tube," in: Shock Tubes, Kh. A. Rakhmatullin and S. S. Semenov (eds.) [Russian translation], IL, Moscow (1962).
5. T. V. Bazhenova and L. G. Gvozdeva, Nonsteady Interactions of Shock Waves [in Russian], Nauka, Moscow (1977).
6. S. P. Medevev, A. N. Polenov, B. E. Gel'fand, and S. A. Tsyganov, "Air SW in the sudden expansion of a compressed two-phase bulk-density medium," Fiz. Goreniya Vzryva, No. 4 (1987).
7. G. N. Suntsov, "Piezoelectric pressure sensor," in: Inform. listok o nauch. tekhn. dostizhenii, No. 82-0281, VIM, Moscow (1982).
8. Ya. T. Zagorskii, Transistorized Measurement Amplifiers [in Russian], Énergiya, Moscow (1971).
9. M. K. Berezkina and I. V. Plotnikov, "The utilization of lithium sulfate pressure-pulse converters in a gasdynamic experiment," Fiz. Goreniya Vzryva, No. 6 (1982).
10. D. Holder and D. Schultz, The Operating Time and Flow Parameters of a Hypersonic Shock Wave, Issled. Giperzvukov. Tech., F. R. Riddel (ed.) [Russian translation], Mir, Moscow (1964).
11. K. P. Stanyukovich, The Nonsteady-State Motion of a Continuous Medium [in Russian], Nauka, Moscow (1971).